

Carbonate Diagenesis in Miocene Sediments from CRP-1, Victoria Land Basin, Antarctica

M. CLAPS¹ & F.S. AGHIB²

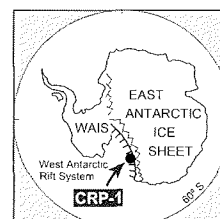
¹Istituto di Scienze del Mare, Università di Ancona, Via Breccie Bianche, Ancona, I-60131 - Italy

²Dipartimento di Scienze della Terra, Università di Milano, Via Mangiagalli 34, Milano, I-20133 - Italy

Received 21 July 1998; accepted in revised form 15 October 1998

Abstract - Preliminary investigation of diagenetic features in Miocene sediments from drill core CRP-1, Victoria Land Basin (Antarctica) shows that carbonate precipitation and cementation occur in various lithologies, particularly in sand-rich portions, such as sandstones, siltstones and diamictites.

Carbonate diagenesis commonly occurs in association with shell material. It is represented by authigenic calcite and siderite, both of which precipitated from grain surfaces and formed rims within intraparticle cavities and voids of skeletal fragments. The carbonates are often found closely related to cryptocrystalline concretions and framboidal crystals of pyrite. Carbonate precipitation and cementation in CRP-1 sediments seem to be controlled by selective dissolution of biogenic aragonitic skeletal tests and favourable conditions provided by organic matter degradation.



INTRODUCTION

The CRP-1 drillhole is located about 16 km offshore Cape Roberts, Ross Sea (Antarctica), between the margin of the Victoria Land Basin and the Transantarctic Mountain Front. The upper part of the drilled sequence, approximately above 43 mbsf (metres below sea floor), are interpreted to be Quaternary in age. They are separated by an unconformity from the lower section, consisting of glacial lithified sediments of early Miocene age (Cape Roberts Science Team, 1998a).

Descriptions of diagenetic features in Miocene marine sediments from Antarctica, in particular from the Victoria Land Basin, are quite rare in the scientific literature, except for the research carried out on the CIROS-1 core by Bridle & Robinson (1989) and on the CRP-1 core by Baker & Fielding (this volume).

Therefore, in this paper preliminary results on carbonate cementation and concretion are presented, on the basis of selected samples from the early Miocene portion of CRP-1 core.

MATERIAL ANALYSED AND METHODOLOGY

The material studied is derived from two main lithologies: (i) lithified, uncemented fine-grained sandstones and siltstones (common in the upper portion, 46-61 mbsf), and (ii) lithified uncemented muddy diamictites (mainly from the lower portion, 112-139 mbsf) (Fig. 1). No samples are available from the intermediate interval.

In these two lithologies, carbonate concretions and authigenic carbonates have been observed. The sediment matrix normally contains detrital quartz, feldspar, clay and

Fe-Mg-rich minerals (amphibole, olivine and pyroxene). Occasionally, small mudstone clasts and fossil fragments were found.

Samples were first impregnated, and then thin sections prepared for sedimentological and textural observations. The sections were later polished and coated with gold/carbon for scanning electron microscope (SEM) and energy dispersive system (EDS) investigations. Ultratextural and compositional analyses were performed at the *Dipartimento di Scienze della Terra* of Milan University using a Cambridge Stereoscan 250 attached to an EDS Link AN10000, and at the *Dipartimento di Scienze della Terra* of Siena University using a Philips XL30 coupled with an EDAX DX4.

DESCRIPTION OF SELECTED SAMPLES

Sample 46.10-46.15 mbsf (lithostratigraphic Unit 5.1) consists of a lithified, moderate to well-sorted, fine-grained sandstone concretion. Polychaete worm tubes, 1 to 2 mm in diameter, are present (Fig. 2a & b). Carbonate cements occur as calcite and siderite rims associated with skeletal material (both complete or fragmented shells, Fig. 2a & b): the calcite precipitation is followed by the formation of the siderite rim. The sandy fraction is dominated by fine and very fine-grained quartz, with subangular to subrounded grains. Volcanic rock fragments, feldspar, amphibole, olivine and fragments of volcanic glass occur in trace amounts. Microcrystals and framboids of pyrite are present. Occasionally diatoms and sponge spicules occur.

Sample 59.26-59.29 mbsf (lithostratigraphic Unit 5.2) consists of lithified, poorly to moderately sorted, fossiliferous siltstone. Small mudstone clasts are dispersed

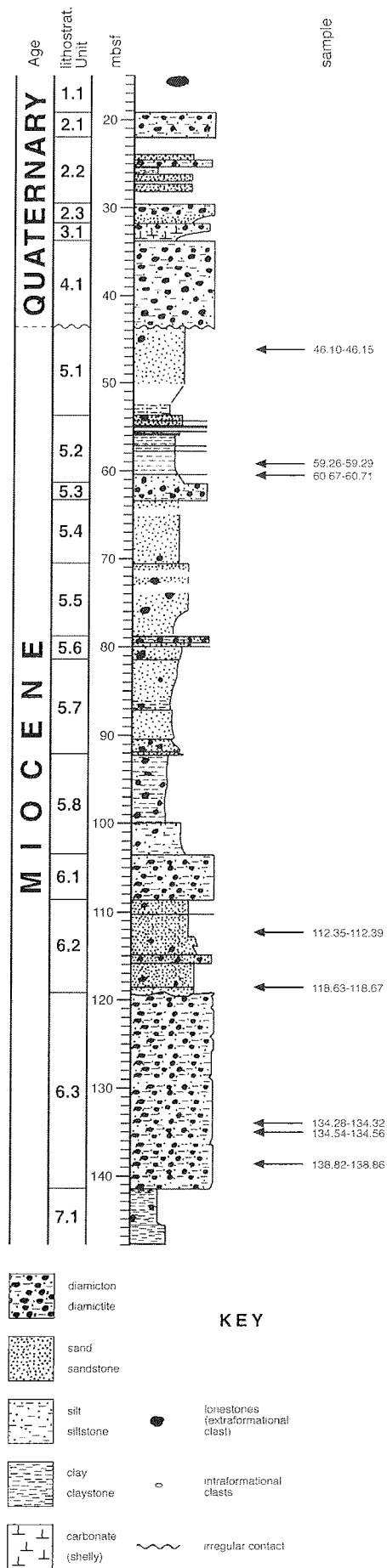


Fig. 1 - Lithostratigraphic column with lithostratigraphic subdivisions (after Cape Roberts Science Team, 1998a), showing the positions of the samples studied.

throughout the sample. Sand-size grains consist mainly of quartz, rock fragments (mostly volcanic) and feldspar. Carbonate cementation occurs as calcite microconcretions rimmed by a thin siderite fringe (Fig. 3a).

Sample 60.67-60.71 mbsf (lithostratigraphic Unit 5.2) consists of lithified, poorly-sorted fine-grained sandstone (rarely siltstone) with scattered small mudstone clasts. The main components are quartz (dominant), feldspar, pyroxene, amphibole and rock fragments. Skeletal fragments (diatoms, sponge spicules) are rare. Carbonate cements were not recognised.

Sample 112.35-112.39 mbsf (lithostratigraphic Unit 6.2) consists of lithified, poorly to moderately sorted, fine to coarse sandstone. Repeatedly, it appears black in colour, because of the presence of organic matter. Thin dark lenses of silty claystone with associated pyrite micrograins alternate with sandstones. Quartz grains are dominant, while volcanic rock fragments, feldspar and feric minerals are subordinate. Thin rims of cryptocrystalline carbonate cement occur around quartz grains.

Sample 118.63-118.67 mbsf (lithostratigraphic Unit 6.2) consists of lithified, poorly to moderately sorted, fine to coarse-grained sandstone. Small rounded intraclasts are present. Common components are quartz, feldspar, amphibole and rock fragments. Pyrite micrograins are dispersed within the matrix. Sand-size grains are sometimes enveloped by cryptocrystalline carbonate cement.

Sample 134.28-134.32 mbsf (lithostratigraphic Unit 6.3) consists of lithified, very poorly-sorted muddy diamictite, with irregular lenses of black siltstone, showing various degrees of cementation.

Sample 134.54-134.56 mbsf (lithostratigraphic Unit 6.3) consists of lithified, very poorly-sorted muddy diamictite, with fossiliferous mudstone clasts and dispersed biogenic skeletal material. Carbonate cements were not observed.

Sample 138.82-138.86 mbsf (lithostratigraphic Unit 6.3) is represented by a single, carbonate-cemented, siltstone concretion in a muddy diamictite matrix (Fig. 2c). Principal skeletal components consist of polychaete worm tubes (Cape Roberts Science Team, 1998b). Carbonate cementation is abundant within fossil cavities. The sandy fraction comprises quartz, volcanic rock fragments and feldspar grains. Two agglutinated foraminifera are recognised in the muddy matrix, with chambers partially filled by microcrystalline calcite (Fig. 2d).

DIAGENETIC FEATURES

Ultratexture, precipitation of authigenic carbonates and preservation/dissolution of biogenic tests were evaluated using SEM/EDS backscattered imaging.

The fine-grained sandstones and siltstones are cemented by authigenic calcite which has a very low content of Mg. It occurs as "patchy" carbonates, and as authigenic anhedral calcite crystals around subangular to subrounded quartz grains in siltstones and sandstones (Fig. 3a & b). Carbonate cement is more abundant in a few samples (46.10-46.15 mbsf, 59.26-59.29 mbsf, 138.82-138.86 mbsf) where cryptocrystalline low-Mg calcite, iron-rich carbonates

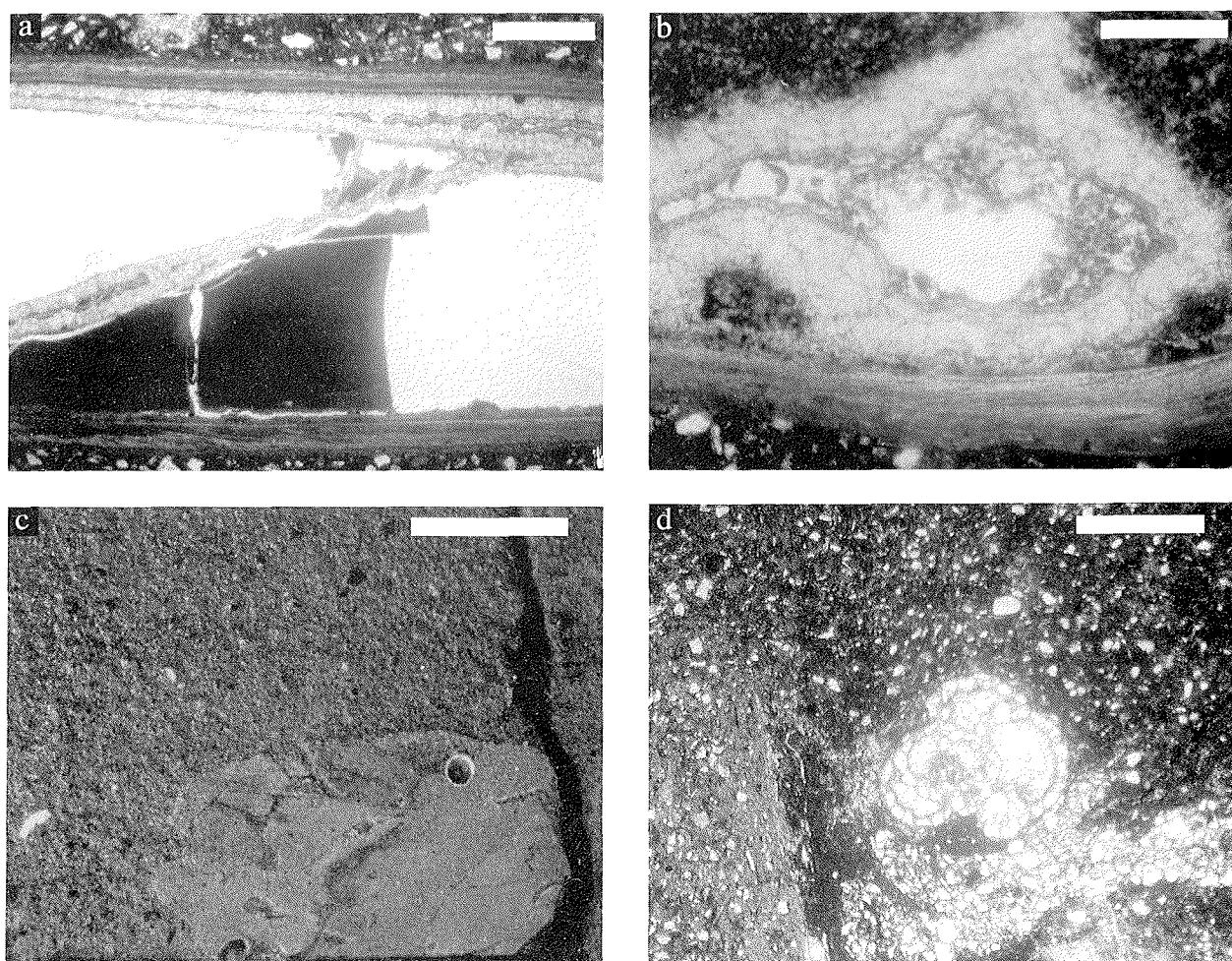


Fig. 2 - *a*) Polychaete worm tube (46.10-46.15 mbsf; scale bar 5 mm) showing the original test still preserved; a first generation of calcitic cement is followed by siderite precipitation within open fractures. *b*) Cavity filled by two generations of cement within a polychaete worm tube (46.10-46.15 mbsf; scale bar 5 mm); the drusy mosaic of calcite microcrystals is interrupted by a thin fringe of siderite. *c*) Polychaete-bearing carbonate concretion from 138.82-138.86 mbsf (scale bar 1 cm). *d*) Agglutinated foraminiferal test with calcite-filled cavities from the carbonate concretion at 138.82-138.86 mbsf (scale bar 5 mm).

and microconcretions of calcite/siderite have been observed as crystal growths a few microns across within the matrix (Figs. 3a, b, 4 & 5). EDS analysis of these small concretions, ranging in size from few microns to as much as 100 μm , shows that they are composed of low-Mg calcite and are surrounded by a thin rim of siderite (Figs. 3a & 5). Tiny pyrite framboids are common and dispersed within the fine-grained matrix (Fig. 3c & d). Biogenic tests are sparse and broken. If present, they consist of polychaete worm tubes (Figs. 2a, b, c & 3d), agglutinated and calcitic foraminifera (Figs. 2d, 3c & e), and fragments of siliceous tests (such as diatoms, Fig. 3f, and sponge spicules).

Polychaete shells, of which only a few have been observed (Figs. 2a, b, c & 3d), consist of low-Mg calcite. Two distinctive generations of calcitic cement have been observed within the polychaete tube: an outer fringe with equant microcrystals rimmed by acicular microcrystals, the latter being characterised by a marked increase in Mg and Fe contents towards the inner area (Fig. 2a). The voids that are not completely filled by these microlayers of cement often display a very thin regular rim of siderite (Fig. 2a & b). This feature is considered to be a late phase of cementation. The fine-grained matrix surrounding the

polychaete worm tube is well cemented by low-Mg calcite forming thin linings around the quartz grains.

The agglutinated foraminiferal tests (Figs. 2d & 3c) are composed of equant quartz grains; the inner voids within the foraminiferal tests show calcitic cement, with variable percentage of Mg and Fe. There is no clear evidence of dissolution on a broken calcitic foraminiferal test, which appears well preserved (Fig. 3e).

DISCUSSION

Cement fringes are more common and better developed in relatively coarse-grained sediments, suggesting a clear relationship between carbonate precipitation and texture. Where the matrix shows an increase in its mud content (as in the diamictite lithotype), carbonate precipitation may be still discernable with energy dispersive analysis, but the presence of clay minerals acts as inhibiting factor and the carbonates are dispersed or occur as thin linings.

The content of carbonate cement is higher where large calcitic shells are present, suggesting a clear association between the occurrence of fossils and the precipitation of

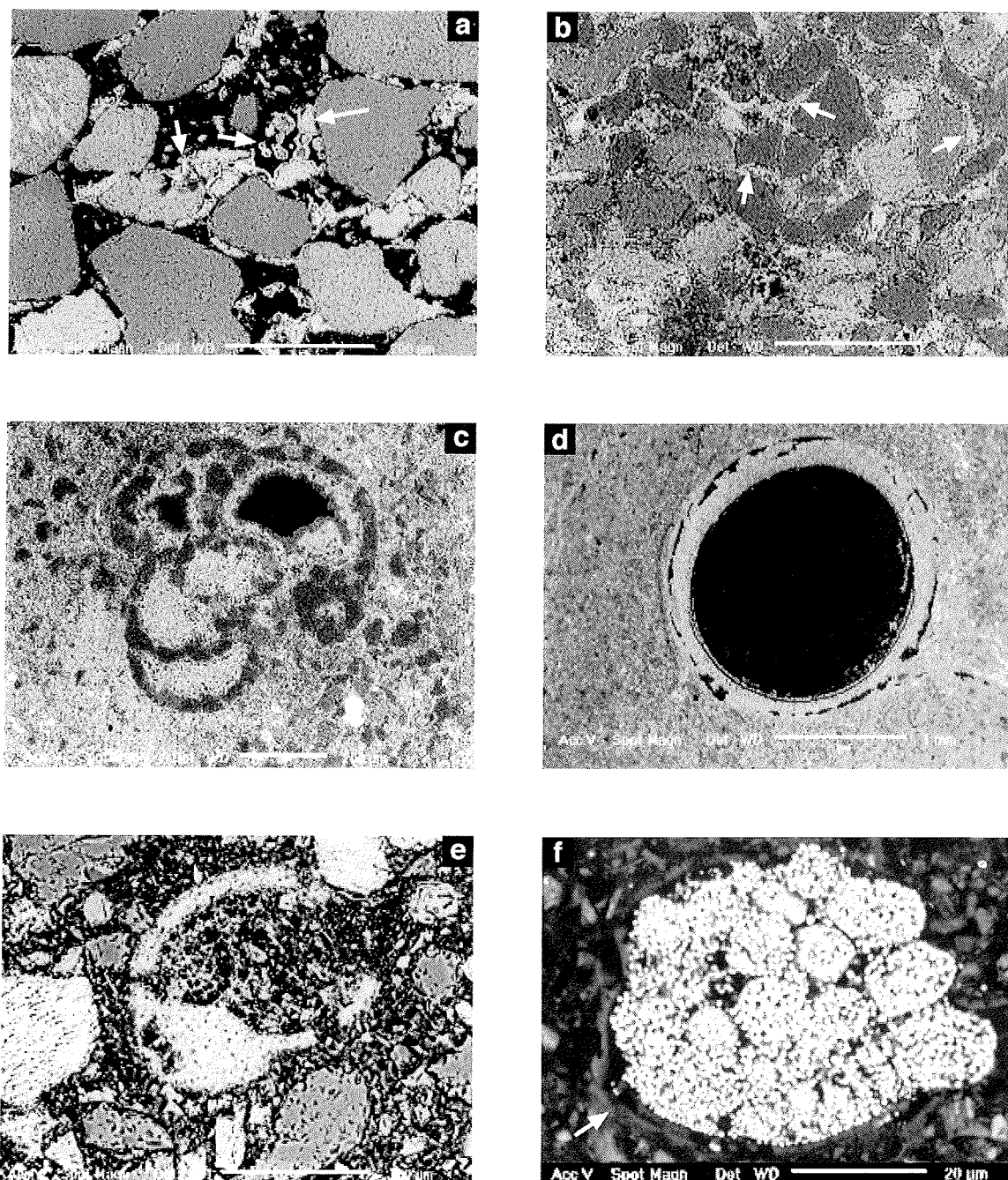


Fig. 3 - Scanning electron micrographs of ultratexture. *a*) Growth of calcite/siderite microconcretions around quartz grains; the arrows point to the microconcretions (59.26-59.29 mbsf; scale bar 200 μ m). *b*) Calcitic cement (arrows) around subrounded to subangular quartz grains and sparse rock fragments (118.63-118.67 mbsf; scale bar 200 μ m). *c*) Agglutinated foraminiferal test within fine-grained matrix with pyrite microcrystals, displayed as bright white dots (138.82-138.86 mbsf; scale bar 200 μ m). *d*) Axial section of a polychaete worm tube displaying layering in the inner calcitic fringe; abundant pyrite microcrystals are dispersed in the fine-grained matrix (138.82-138.86 mbsf; scale bar 1 mm). *e*) Fragment of calcitic foraminifera with no evidence of dissolution (134.54-134.56 mbsf; scale bar 100 μ m). *f*) Pyrite framboids occurring within a diatom test fragment (see arrow; 112.35-112.39 mbsf; scale bar 20 μ m).

carbonate (in the form of concretions, microconcretions and cement rims). Therefore it is assumed that calcitic skeletal fragments act as nuclei for subsequent crystal growth. The degradation of organic matter associated with subsequent sulphate reduction may lead to an increase of both alkalinity and pH in the pore waters, providing the necessary conditions for carbonate precipitation to occur (Raiswell, 1988). Calcium carbonate is the most common cement in the samples studied, as it has been previously described for the CIROS-1 core (Bridle & Robinson,

1989) and for the CRP-1 core (Baker & Fielding, this volume).

A possible source of carbonate-enriched pore fluids could be explained by the dissolution of aragonite and calcite skeletal tests and debris due to undersaturation of CaCO_3 in very cold waters of high-latitude seas (Rao, 1996). The presence of few predominantly calcitic macrofossil remnants (*Chlamys* at 62.19 mbsf and polychaete worm tubes at 46.10-46.15 mbsf and 138.82-138.86 mbsf, Jonkers & Taviani, this volume) and of very

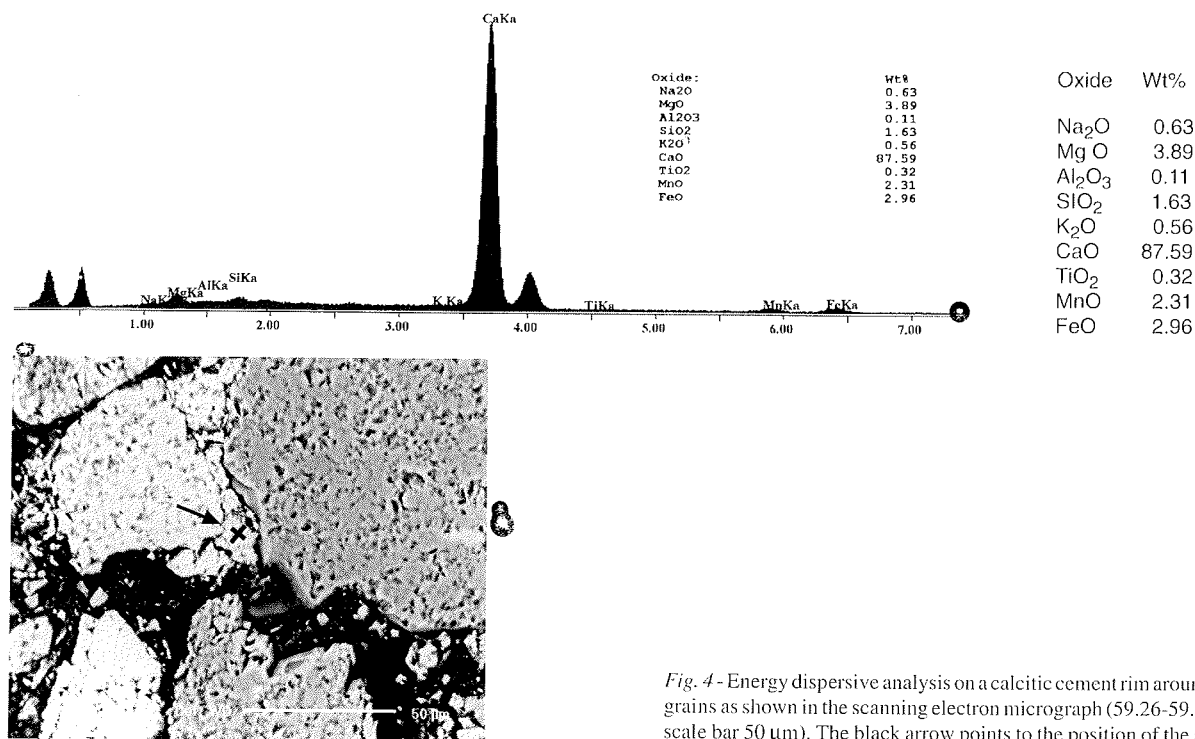


Fig. 4 - Energy dispersive analysis on a calcitic cement rim around quartz grains as shown in the scanning electron micrograph (59.26-59.29 mbsf; scale bar 50 μm). The black arrow points to the position of the analysis.

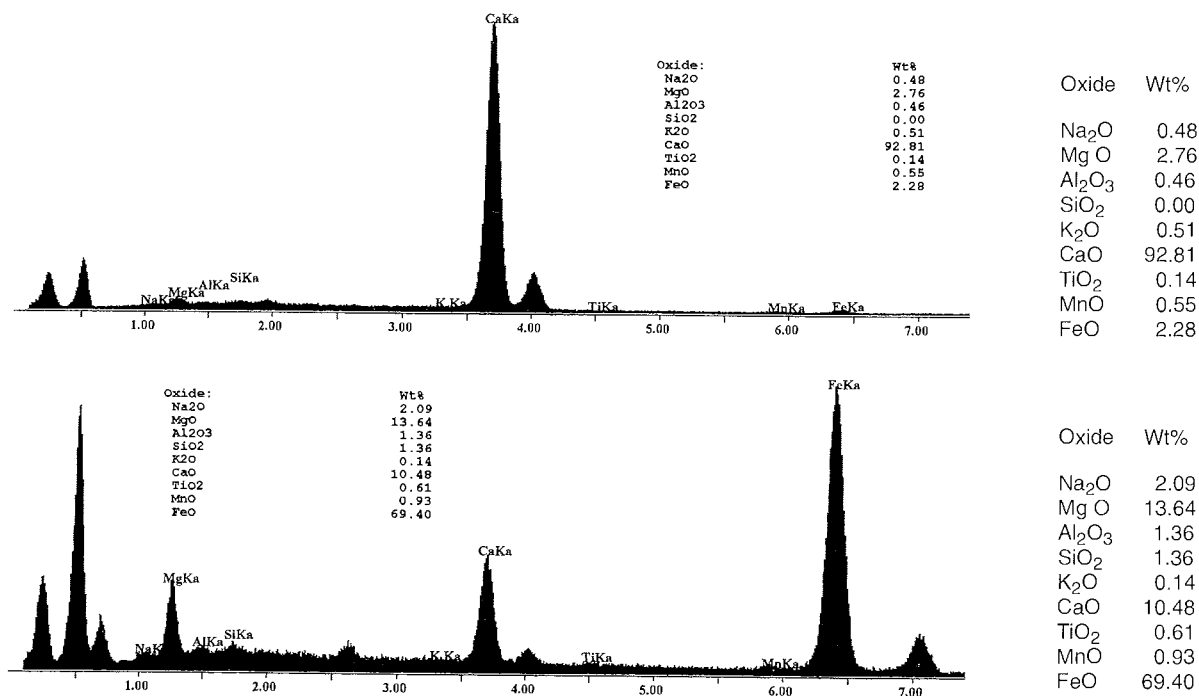


Fig. 5 - Energy dispersive analyses and scanning electron micrograph of calcite/siderite microconcretions (59.26-59.29 mbsf; scale bar 100 μm). The white arrows point to the calcitic nucleus, the black arrows indicate the thin siderite rim around the microconcretions.

rare calcitic foraminiferal tests (see also Strong & Webb, this volume) could support the hypothesis of selective dissolution of calcareous tests (Srivastava, 1975; Canfield & Raiswell, 1991). The aragonitic tests are preferentially removed relative to the large and resistant calcitic ones, which often show well preserved external ornamentation and no evidence of corrosion (Cape Roberts Science Team, 1998b).

In cases where sufficient iron is available in the system, anaerobic bacterial decomposition of organic matter results in sulphate reduction and precipitation of pyrite (Fig. 3c, d & f). If the concentration of iron reaches very high values, Fe-rich calcite can precipitate as cement both around grains and along walls of cavities (Figs. 2a, b & 3c). Siderite occurring as rims along previously precipitated calcite crystals (Fig. 2a & b) and around calcitic microconcretions (Figs. 3a & 5) documents an early stage of diagenetic replacement of calcite after pyrite precipitation was completed (Berner, 1971). The occurrence of authigenic Fe-Mn carbonate nodules have been also reported at DSDP Site 603 on the North American continental rise by von Rad & Botz (1987).

The investigation of diagenetic features of the early Miocene sediments from the CRP-1 core suggests the following trend of authigenic carbonate formation: (i) low-Mg calcite precipitation with a gradual increase in Fe content in form of microconcretions and cements, and (ii) siderite precipitation as thin rims during an early diagenetic stage.

ACKNOWLEDGEMENTS

The authors are grateful to the Cape Roberts Science Team whose advice and suggestions helped the completion of this

contribution. P.J. Barrett, M. Taviani and M. Sarti are particularly acknowledged for fruitful discussions and for focusing on important aspects of the study. The authors are deeply indebted to C.A. Ricci who provided facilities at University of Siena. An early version of the manuscript benefitted from the review of M.B. Cita. We thank M. Feldman, P.H. Robinson, W. Ehrmann and M. Hambrey for very careful review and for improving the English text. We wish to thank C. Malinverno for technical support in thin section preparation, and A. Rizzi and C. Viti for SEM/EDS investigation. Financial support for this study was provided by the Italian *Programma Nazionale di Ricerche in Antartide* (PNRA) and MURST 40% (M. Sarti).

REFERENCES

- Berner R.A., 1971. *Principles of Chemical Sedimentology*. McGraw Hill, New York, 192-200.
- Bridle I.M. & Robinson P.H., 1989. Diagenesis. In: Barrett P.J. (ed.), *Antarctic Cenozoic history from the CIROS-1 drillhole, McMurdo Sound, DSIR Bulletin*, **245**, 201-207.
- Canfield D.E. & Raiswell R., 1991. Carbonate precipitation and dissolution. In: Allison P.A. & Briggs A.E. (eds.), *Taphonomy: releasing the data locked in the fossil record*, Plenum Press, New York, 411-453.
- Cape Roberts Science Team, 1998a. Background to CRP-1, Cape Roberts Project, Antarctica. *Terra Antarctica*, **5**(1), 1-30.
- Cape Roberts Science Team, 1998b. Miocene strata in CRP-1, Cape Roberts Project, Antarctica. *Terra Antarctica*, **5**(1), 63-124.
- Raiswell R., 1988. Evidence for surface-reaction controlled growth of carbonate concretion in shales. *Sedimentology*, **35**, 571-575.
- Rao C.P., 1996. *Modern Carbonates: tropical, temperate, polar*. Arts of Tasmania, Hobart, 206 p.
- Srivastava N.K., 1975. Early diagenetic changes in Recent molluscan shells. *Neues Jahrb. Geol. Paläontol. Abh.*, **148**, 380-403.
- von Rad U. & Botz R., 1987. Authigenic Fe-Mn carbonates in Cretaceous and tertiary sediments of the continental rise off eastern North America, Deep Sea Drilling Project Site 603. In: van Hinte J.E. et al. (eds.), *Initial Report of the Deep Sea Drilling Project*, U. S. Govt. Printing Office, Washington D.C., 1061-1077.